Special Issue on "Medicinal Chemistry"

J. Indian Chem. Soc.,
Vol. 97, August 2020, pp. 1199-1209

Functionalized sulfamethoxazole and its metal complex : Structural characterization, antibacterial and anticancer study of sulfamethoxazolyl-azo-salicylic acid and its copper(II) complex

Nilima Sahu[a], Kunal Pal[b], Faruk Ahmed[a], Nayim Sepay[a], Kuladip Jana[b], Alexandra M. Z. Slawin[c] and Chittaranjan Sinha*[a]

[a]Department of Chemistry, [b]Department of Life Science and Biotechnology,

Jadavpur University, Kolkata-700 032, India

[c]School of Chemistry, University of St Andrews, Purdie Building, North Haugh, St Andrews Fife Scotland, KY16 9ST, UK

E-mail: crsjuchem@gmail.com

Manuscript received online 30 June 2020, accepted 28 July 2020

Sulfamethoxazolyl-azo-salicylic acid, SMX-N=N-C_6H_3(*p*-OH)(*m*-COOH) (**1**) and its Cu(II) complex, Na_2[Cu(SMX-N=N-C_6H_3(*p*-O)-(*m*-COO))$_2$].4H_2O (**2**) are structurally characterized by different spectroscopic data. The single crystal X-ray structure of **1** shows inter- and intra-molecular hydrogen bonds and π---π interactions and has constituted 1D chain. The optimized structure of **2** is optimized by theoretical computation. The compounds, **1** and **2**, show better antimicrobial activity to *S. aureus* (Gram-positive bacteria) and *E. coli* (Gram-negative bacteria) relative to the drug SMX and follow the order SMX < **1** < **2**. The IC_{50} data of *S. aureus* are 320.2 μg/ml (SMX), 210.1 μg/ml (**1**), 150.2 μg/ml (**2**) and that of *E. coli* are 300.1 μg/ml (SMX), 200.0 μg/ml (**1**), 147.2 μg/ml (**2**). The compounds, **1** and **2**, also exhibit promising anticancer activity against human breast cancer cells, MDA-MB 468 and the LD_{50} values are 63.00 (**1**), 65.00 (**2**) μM. The electronic and spectral properties have been explained by DFT and TD-DFT data. *In silico* Molecular Docking is analyzed to determine the most favorable binding site of minimum free energy of the drugs with the active site residues of DHPS (dihydropteroate synthetase).

Keywords: Sulfamethoxazolyl-azo-salicylic acid, X-ray structure, Cu(II) complex, antibacterial properties, anticancer activity, theoretical computation.

Introduction

The antibiotics either kill or inhibit the growth of microbes[1,2]. Penicillin discovered by Alexander Fleming in 1928 is the first antibiotic and is effective against a wide range of infectious microorganism including fungi and protozoa[3,4]. Sulfonamides, class of synthetic antibiotic, also help insulin releasing[5], anti-inflammatory[6] and anti-tumor[7] agents. Sulfamethoxazole (SMX), an inhibitor to folate biosynthesis in the microorganisms, acts as a competitive antagonist of *p*-amino benzoic acid (PABA) in the DHPS (dihydropteroate synthase) activity. Some of the metabolic intermediates of sulfamethoxazole are highly toxic, such as SMX-hydroxylamine (SMX-NHOH) and SMX-nitroso (SMX-NO)[8–10]. The toxicity may be arrested/minimized by the functionalization of *p*-NH_2 group of sulfamethoxazole via diazotization or Schiff base formation[11–13].

Both the sulfonamide Schiff bases and azo compounds are important in pharmaceuticals and medicinal chemistry[14,15]. It is reported that the derivatives of sulfonamides and their metal complexes are more efficient and less toxic drugs than precursors[11,12,16]. It is the source of motivation to search for metallo-drugs of sulfonamides of low toxicity and more effective than that of parent drug[11,16]. In this work, we have functionalized sulfonamide-azo-salicylic acid derivative and have examined their drug efficiency. Salicylic acid, a keratolytic (peeling agent), is analgesic (pain relieving) and antipyretic (anti-inflammatory) and occurs naturally in certain plants, including wintergreen leaves, sweet birch bark

and willow bark. This prompts us to append salicylic acid to sulfamethoxazole by azo (-N=N-) function in a single molecule and to examine its biomedical efficiency.

Transition metal complexes, d-block and f-block metal ions, have useful applications as therapeutic agents[12–16]. The biological role and synergetic activity of copper(II) with the drugs are very important[15]. *N*-(2-Hydroxy-5-(4-(*N*-(5-methylisoxazol-3-yl)sulfamoyl)phynyl)diazenyl)phenyl) benzoic acid (SMX-N=N-C_6H_3(*p*-OH)(*m*-COOH)) (**1**) and Cu(II) complex, Na_2[Cu(SMX-N=N-C_6H_3(*p*-O)-(*m*-COO))$_2$].4H_2O (**2**) are characterized and biological activities are evaluated.

The structural confirmation of **1** has been examined by single crystal X-ray diffraction data along with other physicochemical data. The DNA interaction of **1** and **2** has been carried out by spectroscopic experiments. Electronic properties have been evaluated by DFT and TD-DFT computation. *In silico* molecular docking is also studied with DHPS protein (obtained from PDB source) and best DNA pose condition of the compound is determined.

Experimental

Materials and methods:

Sulfamethoxazole purchased from Hi-Media; $NaNO_2$, NaOH were available from S.D. Fine Chem. Ltd.; salicylic acid, $CuCl_2.2H_2O$, thiazolyl blue formazan (MTT), were purchased from Sigma Aldrich, cell culture media, DMEM, Fetal Bovine Serum (FBS), were procured from Invitrogen-Life Technologies and other chemicals and solvents were reagent grade and had been purified by standard procedure[17].

Physical measurement:

Perkin-Elmer 2400 CHNS/O elemental analyzer was used for microanalytical data (C, H, and N) collection. Spectroscopic data were obtained by the following instruments: Perkin-Elmer FT-IR spectrophotometer model RX-1 for infrared spectra (KBr disk, 4000–400 cm^{-1}); Perkin-Elmer UV-Vis spectrophotometer model Lambda 25 employed for UV-Vis spectra collection. The ^{1}H NMR spectra were recorded by Bruker (AC) 300/500 MHz FTNMR spectrometer and ESI mass spectra were recorded on a micro mass Q-TOF mass spectrometer (Serial no. YA 263). Magnetic susceptibility measurement of a powder crystalline sample of **2** were carried out at Sherwood Scientific Magnetic Susceptibility Balance model Mk1 at 300 K and the data were corrected by using diamagnetic corrections from Pascal's Tables[18]. The EPR spectrum was carried out at 298 K and 77 K by an X-band (9.15 GHz) Varian E-9 spectrometer. Thermal study had been carried out by using DTG-60H, Shimadzu, Japan within 25–600°C at the rate 10°C per minute. Nanoparticle was determined by dynamic light scattering experiment using a Malvern Zetasizer (NanoZS90, Malvern Instruments Limited, Worcestsershire, UK) and surface charge of the nanoparticle was measured by Malvern Zetasizer (Nano ZS90, Malvern Instruments Limited, Worcestsershire, UK). Iodometric estimation of copper in the complex **2** was followed by literature method[15].

Synthesis:

*Synthesis of SMX-N=N-C_6H_3 (p-OH)(m-COOH) (**1**):*

Sulfamethoxazole (0.5 g, 1.97 mmol) in acid solution (3*N* HCl, 20 ml) was reacted with aqueous cold sodium nitrite (0.15 g, 2.17 mmol, 5 ml) with stirring at 0–5°C for 20 min to synthesize sulfamethoxazolyl-diazonium (SMX-N=N-$^+$) ion and the solution was then added in drops to cold alkaline (2.4 g, NaOH) solution of salicylic acid (0.343 g, 1.97 mmol). A yellow precipitate appeared at pH 7 and was filtered, washed with water and dried *in vacuo*. The product was crystallized from hot aqueous-methanol (2:1, v/v) mixture. Needle shaped bright crystals were separated. Further purification was done by column chromatography (silica gel, 60–120 mesh) and the desired product was eluted with chloroform-ethylacetate (9:1, v/v) mixture. Slow evaporation of orange eluent had separated crystals; yield 78% (0.62 g), m.p. 214°C.

Microanalytical data of SMX-N=N-C_6H_3(*p*-OH)(*m*-COOH) (**1**) ($C_{17}H_{14}N_4O_6S$); MWt. 402.38, Calcd. : C, 50.74; H, 3.51; N, 13.92; Found : C, 50.92; H, 3.47; N, 13.78%. Mass spectra $(M+Na)^+$ (*m/z*), 425.06 (Supplementary Materials, Fig. S1). FT-IR (KBr disk; ν, cm^{-1}): ν(COO), 1663; ν(N=N), 1472; ν(C=N), 1617; ν(O-H), 3168; ν(S=O), 1171; ν(S-N), 673 (Supplementary Materials, Fig. S2). ^{1}H NMR spectral data (DMSO-d_6): δ(16-CH_3)(oxazolyl), 2.28 (s); δ(1-OH), 12.58 (s); δ(3-OH), 11.59 (s); δ(N-H), 6.16 (s); δ(4-H), 7.13 (d, *J* 9.21 Hz); δ(5-H), 8.00 (d, *J* 9.78 Hz); δ(7-H), 8.06 (s); δ(10,12-H), 8.03 (m); δ(9,11-H), 8.35 (m); δ(15-H), 7.26 (s) ppm (Supplementary Materials, Fig. S3). UV-Vis absorption spectrum (MeOH, λ/nm (10^3 ε, M^{-1} cm^{-1})) 263 (13.87), 356 (24.18) (Supplementary Materials, Fig. S4). pK_a of the compound is 5.98 (Supplementary Materials, Fig. S5)[19].

*Synthesis of Na_2[Cu(SMX-N=N-C_6H_3(p-O)-(m-COO))$_2$]. 4H_2O (**2**):*

To $CuCl_2.2H_2O$ (0.045 g, 0.26 mmol) solution 0.01 *M* (NaOH) (10 ml) was added followed by the solution of SMX-N=N-C_6H_3(*p*-OH)-(*m*-COOH) (**1**) (0.162 g, 0.40 mmol) in methanol (20 ml) and stirred in air for 2 h. A greenish brown precipitate filtered and purified by slow evaporation of water-methanol (1:9, v/v) mixture and was collected and dried in silica gel blue desiccators. Yield 62% (0.158 g).

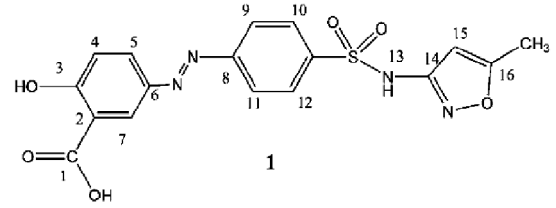

1

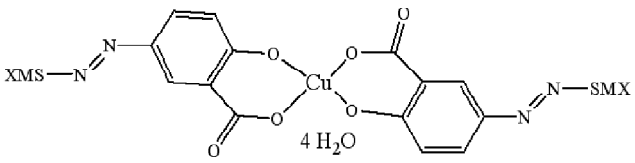

2

Physicochemical data of copper complex:

Na_2[(SMX-N=N-C_6H_3(*p*-O)-(*m*-COO))$_2$Cu].4H_2O(**2**), $Na_2[Cu(C_{34}H_{32}N_8O_{16}S_2)]$ Mwt. 981.66; Calcd. : Cu, 6.47; C, 41.56; H, 3.29; N,11.41; Found : Cu, 6.33; C, 41.41; H, 3.17; N, 11.25%; FT-IR (KBr disk; ν, cm^{-1}): ν(C-O), 1128; ν(N=N), 1471; ν(C=N), 1605; ν(O-H_2), 3424; ν(S=O), 1174 (Supplementary Materials, Fig. S6). UV-Vis spectrum (water, λ/nm (10^3 ε, M^{-1} cm^{-1})) 267 (17.45), 368 (35.90), 464 (11.44) (Supplementary Materials, Fig. S7). Magnetic moment (μ), 1.64 BM, molar conductance (Λ_M) at 25°C is 200.4 mho cm^{-2} M^{-1}. TGA determines thermal stability (Supplementary Materials, Fig. S8) of **2**.

*X-Ray crystal structure determination of SMX-N=N-C_6H_3 (p-OH)(m-COOH) (**1**):*

Two types of crystals were isolated from two different preparatory processes; slow evaporation of methanol-aqueous solution for a week separated a crystal, **1**, of size 0.18×0.17×0.08 mm^3 and diffusion of hexane to dichloromethane solution separated crystal, **1′**, of size 0.20×0.16×0.12 mm^3. Bruker Smart CCD Area Detector was used (1.66 ≤ θ ≤ 25.47 (**1**) at 178 K; 1.00° ≤ θ ≤ 25.38° (**1′**) at 293 K) to collect data. Graphite-monochromatized Mo-Kα radiation (λ = 0.71073 Å) source from fine-focus sealed tube was used. The SADABS program corrected the empirical absorption correction in the *h k l* range: $-8 \le h \le 8$; $-15 \le k \le 15$; $-15 \le l \le 15$ (**1**) and $-6 \le h \le 6$, $-27 \le k \le 27$, $-21 \le l \le 21$ (**1′**)[20] using multi-scan absorption correction process[21]. The SHELXS-97[22,23] program by direct method was used to solve the structure of the crystals and refined by full-matrix least-squares techniques on F^2 using with anisotropic displacement parameters for all non-hydrogen atoms. For crystal **1′**, crystallographic software package except for refinement was executed using SHELXL Version 2014/7[24,25]. Neutral atom scattering factors were taken from International Tables for Crystallography (IT), Vol. C, Table 6.1.1.4[26], anomalous dispersion effects were included in F_{calcd}[27] and the values for $\Delta f'$ and $\Delta f''$ were those of Creagh and McAuley[28]. The values for the mass attenuation coefficients were those of Creagh and Hubbell[29]. All calculations were performed using the Crystal Structure[30]. The structures were solved by direct methods and expanded using Fourier techniques. The non-hydrogen atoms were refined anisotropically. Hydrogen atoms were refined using the riding model. Figures and Tables were prepared with the help of ORTEP-3[31] within WinGX frame. Crystallographic refinement data are collected in Table 1.

*DNA interaction studies with SMX-N=N-C_6H_3(p-OH)(m-COOH) (**1**) and Cu(II) complex (**2**):*

The stock solution of **1** was prepared by dissolving in MeOH where as the solution of **2** were prepared in water and diluting by Tris-HCl buffer. The spectral titration experiment was performed by fixed concentration of ligand or complex with varying the CT-DNA concentration in the UV-Vis spectrophotometer (Perkin-Elmer model Lambda 25). The elimination of the absorbance of DNA was done by itself, equal solution of CT-DNA was added both to the compound solution and to the reference one.

Preparation of calf thymus DNA:

For the experiment of CT-DNA, Tris-HCl buffer solution (pH 8.0) was prepared by using deionized and sonicated HPLC grade water (Merck). The CT-DNA was sufficiently free

Table 1. Crystal data and structure refinement

	1	**1′**
Formulae	$C_{17}H_{14}N_4O_6S.H_2O$	$C_{17}H_{14}N_4O_6S$
Crystal system	Triclinic	Monoclinic
Space group	*P*-1	$P2_1/n$
a (Å)	6.3633(9)	5.0056(3)
b (Å)	12.4867(16)	22.7575(15)
c (Å)	12.6761(18)	17.5961(12
α (°)	90.8461(9)	90
β (°)	103.489(9)	92.234(6)
γ (°)	101.754	90
V (Å^3)	956.8	2002.9(2)
T (K)	298	173
Z	2	4
D_{calcd} (mg/m^3)	1.459	1.334
μ (MoK_α) (mm^{-1})	0.218	0.201
λ (Å)	0.71073	0.71075
θ range (°)	1.66–25.47	1.00–25.383
Unique reflections	3489	3627
Refine parameters	266	261
R_1[a] [$I > 2\sigma(I)$]	0.0787	0.0561
wR_2[b]	0.2095	0.2045
Goodness-of-fit	1.079	1.13

[a]$R = \Sigma||F_0| - |F_c||/\Sigma|F_0|$. [b]$wR = [\Sigma w(F_0^2 - F_c^2)/\Sigma w F_0^4]^{1/2}$ are general but *w* are different, $w = 1/[\sigma^2(F_o^2) + (0.0794\ P)^2 + 0.0000P]$ for **1**; $w = 1/[\sigma^2(F_o^2) + (0.1360\ P)^2 + 0.8978\ P]$ for **1′**.

from protein in experiment. The concentration of DNA was determined by measuring extinction coefficient, ε, 6600 L mol^{-1} cm^{-1} at 260 nm[33]. Stock solution of DNA was always stored at 4°C and used within 4 days.

Absorption spectroscopic studies of the complexes in presence of CT-DNA:

DNA titration was performed on a UV-Vis spectrophotometer taking SMX-N=N-C_6H_3(*p*-OH)(*m*-COOH) (**1**) (42.45 μM) with increasing concentrations of CT-DNA (from 0 μM to 43.3 μM) and for Cu(II) complex (**2**) (18.6 μM) with increasing concentrations of CT-DNA (from 0 μM to 17.89 μM). After addition of DNA in solution of **1** and **2** the mixtures were incubated at room temperature for 15 min and scanned at 225–500 nm. In each set of experiment the self-absorption of DNA was eliminated. For scanning of each sample the number of cycle was 2 having cycle time of 5 s at a scan rate 100 nm/min. To calculate ground state binding constant (K_b) between the compounds and CT-DNA the modified Benesi-Hildebrand[34] plot was applied, i.e.

$$A_0/\Delta A = A_0/\Delta A_{max} + (A_0/\Delta A_{max}) \times 1/K \times 1/L_t$$

where $\Delta A = A_0 - A$, ΔA_{max} = maximum change in absorbance, A_0 = maximum absorbance of receptor molecules (without any DNA), A = absorbance of the receptor molecules (in presence of DNA), L_t = concentration of DNA.

Anticancer activity: Cell cytotoxicity assay:

Viability of human triple negative breast cancer cell line, MDA-MB-468 and normal fibroblast cells after exposure to various concentrations of gum acacia nanoparticles, compounds **1** and **2** loaded gum acacia nanoparticles were determined by MTT assay. The cells were seeded in 96-well plates at 1×10^4 cells per well and exposed to NPs at concentrations of 0–100 μM for 24 h. After incubation cells were washed with 1×PBS twice and incubated with MTT solution (450 μg/ml) for 3–4 h at 37°C. The resulting formazan crystals were dissolved in an MTT solubilization buffer and the absorbance were measured at 570 nm by using a spectrophotometer and the value was compared with control cells.

Antimicrobial activity:

The antibacterial activity of the compounds SMX, SMX-N=N-C_6H_3(*p*-OH)(*m*-COOH) (**1**) and Cu(II) complex (**2**) were studied against Gram-positive bacteria*, S. aureaus* and Gram-negative bacteria, *E. coli* standard. Test tubes containing 4 ml of LB broth media was inoculated with overnight cultures of the bacteria and then various concentrations of different minerals (0.2–1.0 mg ml^{-1}) for all three size fractions of SMX, SMX-N=N-C_6H_3(*p*-OH)(*m*-COOH) (**1**) and Cu(II) complex (**2**) were added in each tube. The OD_{600} had been measured in a UV-Visible spectrophotometer. The observed 100% growth for both the bacterial species in absence of test compound had been considered as control. The relative degree of bacterial growth inhibition had been compared by measuring OD at 600 nm and had been calculated under similar experimental condition. The IC_{50} (concentration of test compound required to inhibit the 50% growth of bacteria) had been calculated from the % reduction of bacterial growth in comparison to control.

Computational study: DFT and docking studies:

Using Gaussian 09 software the optimized geometries of the compounds **1** and **2** were computed by the Density Func-

tional Theory (DFT) at the B3LYP level[34,35] and the Gauss View visualization program[36] was employed. For C, H, N, O the 6-31G(d) basis set were used and the LanL2DZ basis set were added for Cu and S with effective core potential[37,38]. The vibrational frequency of the optimized geometries was checked at the local minima and only positive eigen values were used. The B3LYP optimized geometries were also computed following the use of TDDFT (Time-dependent density functional theory) formalism in water adopting CPCM model[39–41] and the Gauss Sum[42] program was used to calculate the fractional contribution of various groups to each molecular orbital.

The DHPS (Dihydroptorat Synthase of *Versiniapestis*, PDB ID 1AJ0) was downloaded from RCSB protein data bank (http://www.pdb.org.) to carry out *in silico* docking. Sulfamethoxazole, 6-hydroxymethylpterin-diphosphate, magnesium ion were co-crystallized with the enzyme. *In silico* docking was studied by Auto Dock 4.2[43]. The crystallied structure of **1** and the optimized structure of **2** were used for interaction with DHPS protein; minimum free energy of protein-ligand complex was investigated and analyzed. The ADMET properties like absorption, distribution, metabolism, excretion and toxicity were predicted for these drugs using the Docking software[44]. Lipinski's rule of five[45,46] protocol was followed to monitor Drug likeness of **1**.

Results and discussion

The ligand and its copper(II) complex:

Sufamethoxazolyl-azo-salicylic acid (SMX-N=N-C_6H_3(*p*-OH)(*m*-COOH) (**1**)) and its Cu(II) complex, Na_2[Cu(SMX-N=N-C_6H_3(*p*-O)-(*m*-COO))$_2$].4H_2O (**2**) are spectroscopically characterized. The complex **2** shows molar conductivity (Λ_M) 200.4 Ω^{-1} cm^2 mol^{-1} and implies the 2:1 conductivity in aqueous solution. Microanalytical data support the composition of the compounds. Mass spectrum of **1** shows molecular ion peak (*m/z*) at 425.06 which corresponds to $(M+Na)^+$ (Supplementary Materials, Fig. S1). Infrared spectrum of ligand (**1**) shows characteristic stretching frequency (1472 ($\nu_{N=N}$), 1663 (ν_{COO}), 1617 ($\nu_{C=N}$) and 1171 ($\nu_{S=O}$) cm^{-1}) (Supplementary Materials, Fig. S2). The ^{1}H NMR spectrum of **1** (DMSO-d_6) is in support of the structure which shows a singlet resonance at 11.59 ppm corresponding to δ(OH) while carboxylic-OH (-COOH) appears at 12.58 ppm; sulfonamide-NH (-SO_2NH-) shows a broad signal at 6.16 ppm. Oxazolyl-CH_3 appears at 2.28 ppm and other aromatic protons appear at 7.10–8.35 ppm (Supplementary Materials, Fig. S3). The UV-Visible spectrum of **1** in methanol shows high intense absorption at 356 nm and pK_a is 5.98 (Supplementary Materials, Fig. S4, Fig. S5). Infrared spectrum of Cu(II) complex shows stretching at 1467 ($\nu_{N=N}$), 1605 ($\nu_{C=N}$), 1590 (ν_{COO}), 1174 ($\nu_{S=O}$) and 1128 cm^{-1} (ν_{C-O}). Transmission frequency of -COO is significantly shifted to lower value from free ligand (**1**) to complex (**2**) (Supplementary Materials, Fig. S6) which implies the coordination to Cu(II). In the complex, Na_2[Cu(SMX-N=N-C_6H_3(*p*-O)-(*m*-COO))$_2$].4H_2O (**2**) intense bands appear at 267 and 368 nm in water along with a weak broad d-d band at 464 nm (Supplementary Materials, Fig. S7). From the TGA data it has been observed that the compound **2** contains four molecules water (Supplementary Materials, Fig. S8). The magnetic moment of the complex is 1.64 BM at 300 K which supports d^9 electronic configuration. The EPR spectrum of **2** at room temperature (298 K) shows g_{II} (2.22) > $g_{\perp}$ (2.02) (g_e, 2.002) with presence of unpaired electron at $d_{x^2-y^2}$ of ground state configuration that support tetragonal structure of **2** (Supplementary Materials, Fig. S9)[47], and stability constant is 7.24×10^4 M^{-2} (Supplementary Materials, Fig. S10). Repeated solution spectra of the complex in water do not show any change or shifting of the band even after two weeks which supports the solution stability of the complex structure.

*Crystal structure description of **1**:*

Molecular structures of SMX-N=N-C_6H_3(*p*-OH)(*m*-COOH).H_2O (**1**) and SMX-N=N-C_6H_3(*p*-OH)(*m*-COOH) (**1′**) with atom numbering schemes are shown in Figs. 1, 2 and selected bond parameters are listed in Supplementary Materials, Fig. S11, Table S1. Single crystal X-ray structure determination reveals that both **1** (with water) and **1′** (without water) are isotypical. Compound **1** crystallizes in the Triclinic space group $P\bar{1}$ with $Z = 2$. Asymmetric unit for both **1** and **1′** show the same kind of connectivity of atoms (Fig. 3) and the only difference is that compound **1** contains one water molecule.

The discrete unit of **1** is self-assembled through face-to-face $\pi\cdots\pi$ interactions between the aromatic rings and edge-

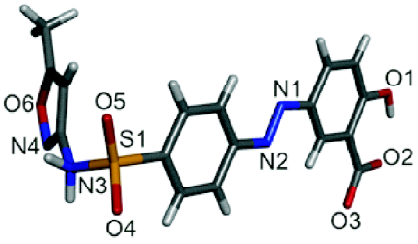

Fig. 1. Asymmetric unit of **1** (N=N, 1.259; O-H, 0.820; S=O, 1.419 Å).

to-face C-H···π interactions between H-atom of the methyl group and aromatic ring of the Schiff base moiety forming 2D network in *ac* plane (Fig. 2). The centroid-centroid distance in case of π···π interactions is 3.824 Å and H-atom to centroid distance is 2.958 Å. Viewing along *a*-axis an interesting pattern of hydrogen bonding has been observed. In the *bc*-plane there are strong N-H···O (N-H, 0.912; H···O, 1.884; N···O, 2.786 Å; ∠N-H···O, 169.84°) and weak S-O···H

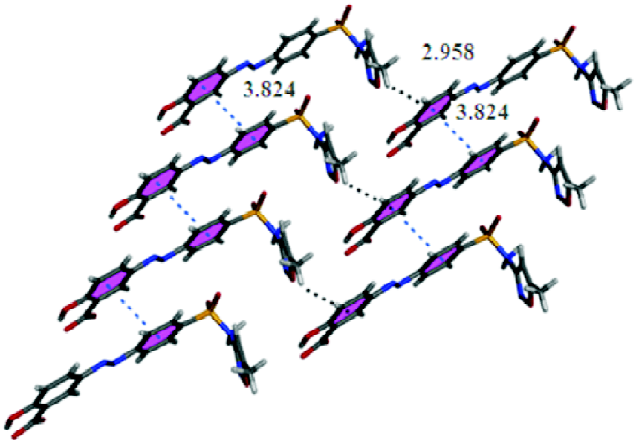

Fig. 2. π···π and C-H···π interactions between the discrete units of **1**.

(S-O, 2.891; O···H, 0.855 Å; S···H, 3.003 Å; ∠S-O···H, 117.86°) hydrogen bonding which are very important in stabilizing the supramolecular assembly. For the fabrication of 3-dimensional (3D) supramolecular assembly, the role of water molecule is very important for compound **1**. Water molecule holds the 2D plane through H-bonds and the O···O separation lies 2.817–2.891 Å (Fig. 4).

The compound **1′** crystallizes in the Monoclinic space group $P2_1/n$ with $Z = 1$, each molecule interacts to an adjacent molecule at either end of itself via strong O-H···N and

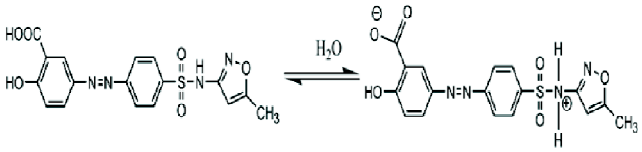

Fig. 3. Conversion of **1′** to **1**.

O···H-N (N-H, 0.880; O···H, 2.070; O···N, 2.667 Å; ∠N-H···O, 155.39°) interactions between the carboxylic acid group and the N atoms on and adjacent to the isoxazole ring. The discrete unit of compound **1′** fabricates 1D zigzag chain through hydrogen bonding (Fig. 4). The N=N bond length of **1** is 1.259(5) Å and comparable with reported data (Table S1). The bond distance of C(13)-N(3), 1.394 Å; N(3)-S(1), 1.626 Å; O(3)-C(17), 1.268 Å; O(2)-C(17), 1.258 Å and bond angles are C(17)-O(3)-O(2), 118.1°; C(13)-N(3)-S(1), 121.0°; O(5)-S(1)-O(4), 120.0°; O(5)-S(1)-N(3), 108.9°; O(4)-S(1)-N(3),103.9° indicate the formation of zwitterion between $-CO_2$ of salicylic acid and $-NH-SO_2$ of SMX. This may suggest the formation of zwitterion in aqueous medium (Fig. 5). Inter-molecular H-bonding between water with $-SO_2-$ (S=O···H-O-H); N of oxazole ring (N···H-O-H, 2.967 Å); O of oxazole ring (O···H-O-H, 3.037 Å); $-CO_2$ of salicylic acid group (C=O···H-O-H, 2.727 and 2.817 Å); and Intra-molecular H-bonding between -COO and -OH (C=O···H-O 2.532 Å) are seen in crystal packing. It is evident that the absence of water molecule impacts the crystal geometry.

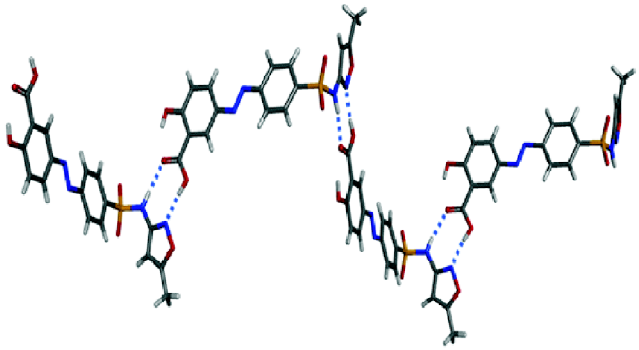

Fig. 4. Formation of 1D zigzag chain through hydrogen bonding in **1′**.

The ligand acts as monoanionic carboxylate bidentate-O,O chelating agent and forms copper(II) complex, $Na_2[Cu(SMX\text{-}N{=}N\text{-}C_6H_3(p\text{-}O)\text{-}(m\text{-}COO))_2].4H_2O$ (**2**) having

cis-orientation. Optimized structure of **2** shows a distorted basal plane of $Cu(O,O)_2$ and fulfill z-out tetragonal geometry (Fig. 5). The Cu-O (acid) 1.937 Å is slightly shorter than Cu-O (O of phenolic -OH) (Cu(1)-O(4), 1.962 Å) bond distances. The chelate angles ∠O-Cu-O lie 87–94° and is closer to square planar bond angle value.

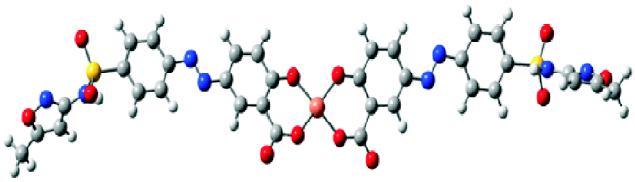

Fig. 5. Optimized structure of $[Cu(SMX\text{-}N{=}N\text{-}C_6H_3(p\text{-}O)\text{-}(m\text{-}COO))_2]^{2-}$ (**2**).

Antibacterial activity:

The compounds, $SMX\text{-}N{=}N\text{-}C_6H_3(p\text{-}OH)COOH$ (**1**) and $Na_2[Cu(SMX\text{-}N{=}N\text{-}C_6H_3(p\text{-}O)\text{-}(m\text{-}COO))_2].4H_2O$ (**2**), have been tested for antimicrobial property against *S. aureus* (ATCC 25923, Gram-positive) and *E. coli* (DH5α, Gram-negative). The IC_{50} of the compounds have been calculated and these are as follows: *S. aureus*: 320.2 μg/ml (SMX), 210.1 μg/ml (**1**), 165.2 μg/ml (**2**); and *E. coli*: 300.1 μg/ml (SMX), 200.0 μg/ml (**1**), 147.2 μg/ml (**2**) (Fig. 6). From the inhibition of bacterial growth of Gram-positive and Gram-negative bacteria, it is clear that the ligand, **1**, and its copper(II) complex (**2**) shows better activity than SMX and follow the sequence SMX < **1** < **2**. Biologically active copper complex has major role in cell immune system. Remarkably, a higher antimicrobial effect against *E. coli* than *S. aureus* is observed. The reason is unclear while the structural difference in bacterial cell walls might be the reason for diffusion. The bacteria cell cover is a complex multilayered structure that assists to protect these organisms from their impulsive and often antagonistic environment. The cell envelopes of most bacteria fall into one of two major groups. A thin negatively charged outer lipopolysaccharide layer of 7–8 nm thickness is encased in Gram-negative bacteria whereas Gram-positive bacterial cell walls is thicker and is composed of highly cross-linked rigid peptidogly can layer (20–80 nm thickness). Thus the Gram-positive cell wall provides higher protection and may inhibit or prevent the bactericidal effect[48].

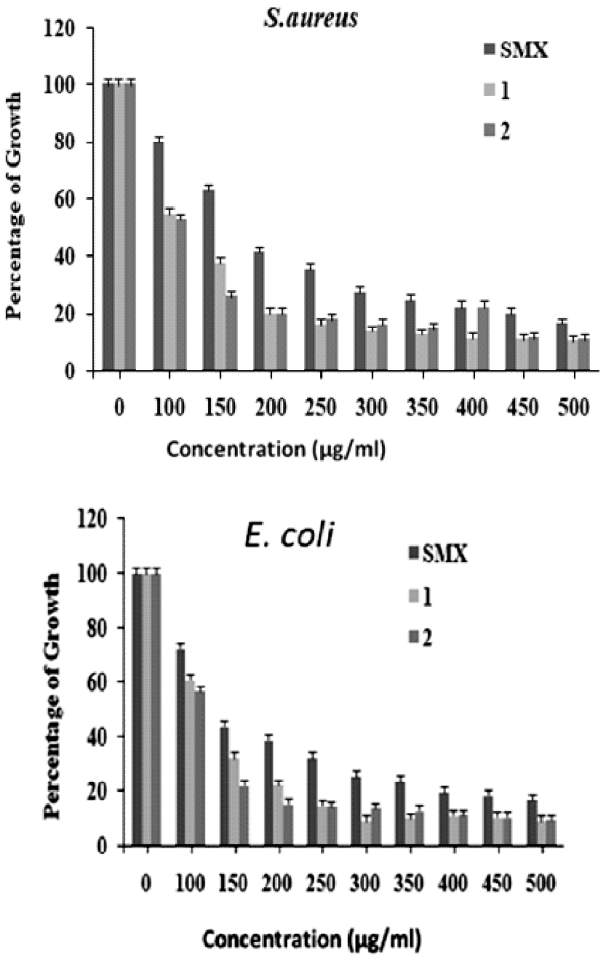

Fig. 6. Inhibition profile of SMX, $[SMX\text{-}N{=}N\text{-}C_6H_3\text{-}(p\text{-}OH)COOH]$ (**1**) and copper complex $Na_2[Cu(SMX\text{-}N{=}N\text{-}C_6H_3(p\text{-}O)\text{-}(m\text{-}COO))_2].4H_2O$ (**2**) for *S. aureus* and *E. coli*.

*Interaction of **1** and **2**, with CT-DNA : Absorption spectroscopic studies:*

Transition metal complexes interact with DNA and has significant role in biology as well as in chemistry. The binding capacity of **1** and **2** with CT-DNA has been studied in absorption spectrophotometer. The binding of compounds with DNA usually results in hypsochromism and a blue shift may be arising from the strong stacking interaction between the compound and DNA[49].

With increasing concentration of CT-DNA to a fixed concentration of **1** and **2** the absorption is increased (Fig. 7 and 8). This characteristic may be due to the specific interaction of the analyte with DNA which is ascends more relax structure of the complex. The binding constant (K_b) is calculated

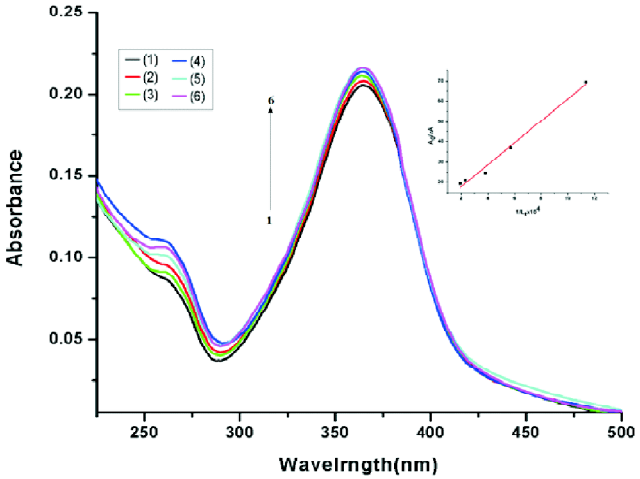

Fig. 7. Absorption spectroscopic study of 42.45 mM SMX-N=N-C_6H_3(*p*-OH)-*m*-COOH (**1**) with increasing concentrations of CT-DNA (0, 8.80, 17.54, 26.22, 34.82, 43.35 µM) respectively (1→6); and modified Benesi-Hildebrand plot for the determination of ground state binding constant between CT-DNA and **1**.

using modified Benesi-Hildebrand plot at the absorption maximum (Figs. 7 and 8) for **1** and **2** and are 3.91×10^4 M^{-1} and 6.861×10^4 M^{-1}respectively.

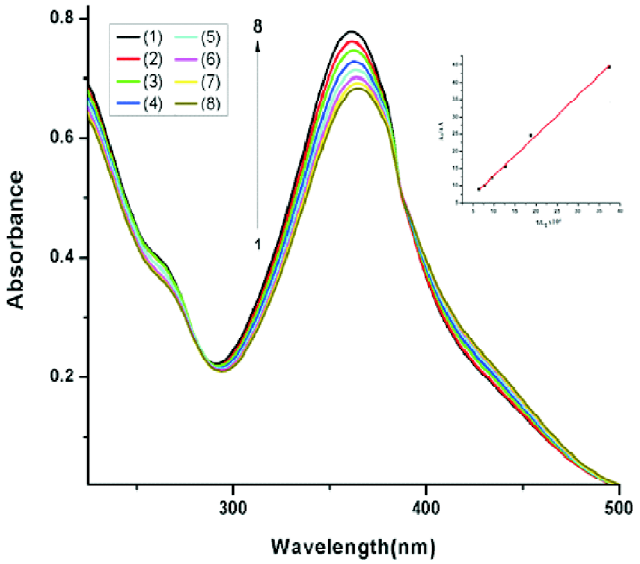

Fig. 8. Absorption spectroscopic study of 18.60 mM Na_2[Cu(SMX-N=N-C_6H_3(*p*-O)-(*m*-COO))$_2$].$4H_2O$ (**2**) with increasing concentrations of CT-DNA (0, 2.67, 5.31, 7.91, 10.46, 12.97, 15.45,17.89 µM) respectively (1→8); and modified Benesi-Hildebrand plot for the determination of ground state binding constant between CT-DNA and **2**.

The drug-DNA interaction is also studied in molecular docking program. The interaction of ligand (**1**) and Cu(II) complex (**2**) with DNA has been recognized through backbone phosphate -O-NH(SO_2NH)- (distance : 2.1–2.9 Å) and significant numbers of C-H···π, π---π interactions. In comparison, the **2** shows higher binding affinity (–7.83 kcal mol^{-1}) towards DHPS protein than that of free ligand (**1**) (–7.07 kcal mol^{-1}). The interaction of base pairs DG16, DA18, DC9, DT19, DG12, DG10 and DG14 of DNA with the complex **2** play the vital role in the interaction activity whereas the base pairs DG22, DT7, DT8, DA5, DC21, DG22 of DNA with the ligand **1** are active in the interaction study (Supplementary Materials, Tables S2, S3 and Figs. 9, 10).

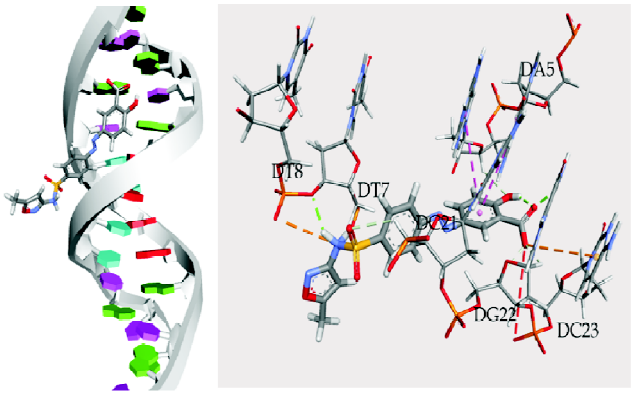

Fig. 9. Best binding mode of **1** in DNA docking.

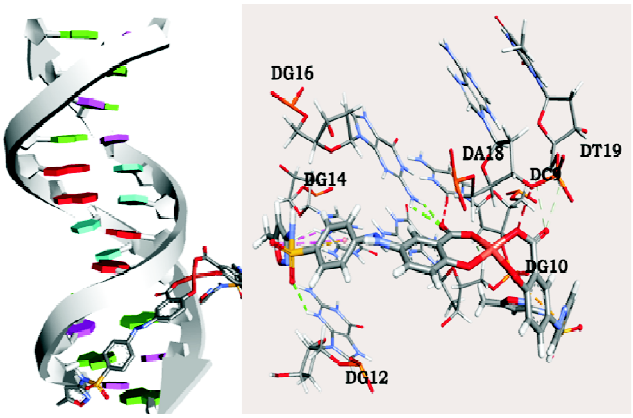

Fig. 10. Best binding mode of **2** in DNA docking.

*Anticancer activity of **1** and **2**:*

Some functionalized sulfonamides possess antibacterial, anti-fungal, diuretic, hypoglycemic and antithyroid activities along with substantial *in vitro* and *in vivo* antitumor activity[50]. Hence two compounds, **1** and **2**, show significant cytotoxic effect in human MDA-MB-468 cell lines. It is found that the cell survivability is decreased in dose dependent manner. The LD_{50} dose of compounds are 63±1.8 (**1**) and 65±2.3 (**2**) (Fig. 11). The mechanism of action has not yet been explored; however, cell cycle blockage via inhibition of protein synthesis may be the reason as the sulfonamide disturbs folate synthetic path.

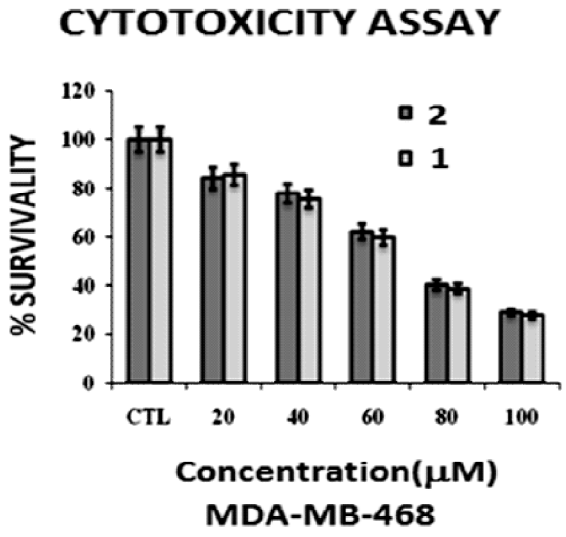

Fig. 11. Cytotoxicity of compounds **1** and **2** against human MDA-MB-468 cell lines.

DFT and docking studies:

The DFT computation technique has been used for the assignment of electronic structure and properties of the **1** and **2**. The optimized structures are used to verify by comparing the bond parameters with X-ray structure of **1** (Table S1). The structure of **1** is constituted by azo, benzene sulfonamide (BA), methyloxazolyl (OX) and salicylic acid (SA) units (Fig. S12). The composition of MOs and proposed electronic transitions in acetonitrile (CH_3CN) solution (Tables S5 and S6) suggest that electron donor parts are salicylic acid molecule and oxazolyl rings while azo function and benzene sulfonamide are electron acceptors. HOMO→LUMO (λ, 384.82 nm; f, 0.0921); HOMO→LUMO+1 (λ, 315.17 nm; f, 0.0505); HOMO-4→LUMO (λ, 289.98 nm; f, 0.0617) transitions are allotted with salicylic acid to azo/benzene sulfonamide charge transferences. In the complex, Na_2[Cu(SMX-N=N-C_6H_3(*p*-O)-(*m*-COO))$_2$].4H_2O (**2**) the composition of HOMO-1 differs significantly with inclusion of copper function (7%; Fig. S13; Tables S7–S8). On comparing with free ligand, **1**, the energy of MOs in metal complex, **2**, is increased. This is recommended to the electron drifting character of Cu^{2+} in the complex. Thus, absorption bands of **2** are shifted to lower energy region or longer wave length. The observed energy of absorptions are closer to the calculated one in the molecules.

Protein structure of DHPS from *E. coli* (PDB file) is used for docking studies with **1** and **2** using by using Autodock 4.2. The dock score of the compound **1** interacts more strongly than SMX to DHPS protein. A comparative study about the binding of **1** and **2** with protein was done. The compounds **1** and **2** have polar parts to bind with protein through hydrogen bonding and different non-covalent interactions like (C-H···π, π···π). From the Gibbs free energy values (**1** : –6.90 kcal mol^{-1}; **2** : –7.18 kcal mol^{-1}) it is observed that complex **2** has more binding affinity towards protein than ligand **1**. Complex **2** prefers to bind at the outer surface cavity region of the protein 1AJ0 whereas **1** prefers binding cavity (Fig. 12). The DNA efficiency of the complex **2** is also proved higher than the ligand **1**.

The amino acid residue Glu155, Gly239, Ser240, Asp243, Ser240, Try178, Asn173, Asn164 and Arg 165 appear in the environment of DHPS@ **1** moiety. There are amino acid residuesare Arg320, Pro321, Try302, Pro336, Gln 335, Lys72, Try340, Gln65, Asn58, Arg159, Gln55 and Arg61 interact with the copper complex, **2**. The DHPS@ **2** analysis suggests that when ligand binds with DHPS moiety three hydrogen bond oxygen atom of -SO_2, oxazolyl moiety azo-N and phenolic OH of salicylic moiety interact with amino acid residue (Figs. 12 and 13) (Gly239C-H---O′-(SO_2-):H---O, 2.75 Å, and ∠C-H–O, 133°; and Gln155 C-O–H′-(OH of salicylic acid:O···H, 2.11 Å, and ∠C-O···H, 132°; Asn173N-H···Norfoxazole:H···N, 1.80 Å, and ∠N-H···N, 168°; etc. The DHPS@ **2** shows two hydrogen bonds between Gln65N-H–O′-(CO_2 of salicylate) H···O, 2.22 Å, and ∠N-H···O, 139°; Try 340 O-H–O′-(SO_2): H···O, 1.98 Å, and ∠O-H···O, 150°;

Arg320 C-H···O′-(SO_2):H···O, 2.58 Å, and ∠O-H···O, 108° (Table S4). The Lipinski's rule of five[51] is used to determine druglikeness of ligand and log P value is 4.03 whereas the complex does not follow Lipinski's filter due to higher molecular weight and has not tested for ADMET module.

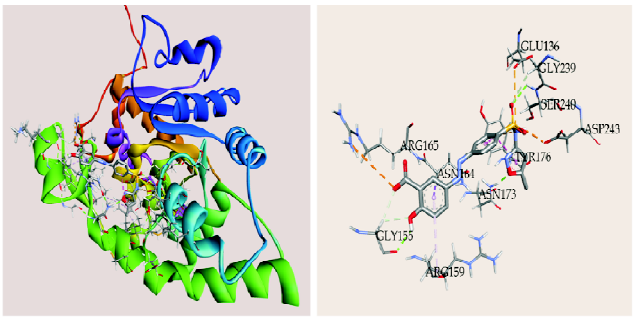

Fig. 12. Best binding mode of **1** in the DHPS (PDB id 3TZF) cavity: (a) 3D interaction and (b) 2D interaction.

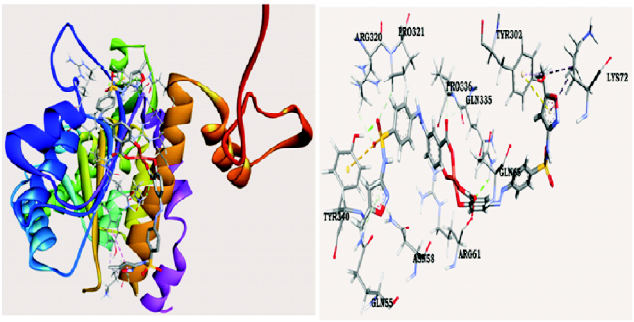

Fig. 13. Best binding mode of **1** in the DHPS (PDB id 3TZF) cavity: (a) 3D interaction and (b) 2D interaction.

Conclusion

Azo-sulfomethoxazolyl-salicylic acid (**1**) and its Cu(II) complex (**2**) are structurally characterized and the antimicrobial activity show better efficiency of the complex, SMX < **1** < **2**. Besides, the complex **2** is less toxic than others. The DNA binding of the compounds are experimentally and theoretically established by *in silico* docking study. The crystal **1** exists in two polymorphic forms in different solvent environment (**1** and **1′**). Furthermore, the compounds possess substantial anticancer activity towards the human breast cancer cell line, MDA-MB-468. The synthesized compounds are endowed with attributes which can be further exploited for application in various fields of biomedical sciences.

Supporting Information

Crystallographic data for the structure have been deposited to the Cambridge Crystallographic Data Center, CCDC No. 1831808 (**1**) and 1564898 (**1′**). These data can be obtained free of charge via http://www.ccdc.cam.ac.uk/conts/retrieving.html, or from the Cambridge Crystallographic Data Centre, 12 Union Road, Cambridge CB2 1EZ, UK; Fax: (+44) 1223-336-033; or E-mail: deposit@ccdc.cam.ac.uk.

Acknowledgements

Financial support from CSIR New Delhi (01(2894)17, EMR-II) and RUSA 2.0 (HRDC, New Delhi supports for infrastructure to Jadavpur University) are thankfully acknowledged. We acknowledge help from Dr. Faruk Ahemed, Department of Chemistry, Aliah University. Infrastructure support to the Department of Chemistry, Jadavpur University.

Reference

1. R. Bentley and J. W. Bennett, *Adv. Appl. Microbiol.,* 2003, **52**, 303.
2. S. B. Singh, K. Young and L. L. Silver, *Biochem. Pharmacol*., 2017, **133**, 63.
3. A. Bult, in: "Metal Ions in Biological Systems", ed. H. Sigel, Marcel Dekker, New York, 1983.
4. F. Zani and P. Vicini, *Arch. Pharm.*, 1998, **331**, 219.
5. T. H. Maren, *Ann. Rev. Pharmacol. Toxicol*., 1976, **16**, 309.
6. J. J. Li, D. Anderson, E. G. Burton, J. N. Cogburn, J. T. Collins, D. J. Garland, S. A Gregory, H. C. Huang, P. C. Isakson, C. M. Koboldt, E. W. Logusch, M. B. Norton, W. E. Perkins, E. J. Reinhard, K. Seibert, A. W. Veenhuizem, Y. Zang and D. B. Reitz, *J. Med. Chem.*, 1995, **38**, 4570.
7. H. Yoshino, N. Ueda, J. Niijma, H. Sugumi, Y. Kotake, N. Koyanagi, K. Yoshimatsu, M. Asada, T. Watanabe, T. Nagasu, K. Tsukahara, A. Lijima and K. J. Kitoh, *J. Med. Chem.,* 1992, **35**, 2496.
8. G. C. Slatore and A. S. Tilles, *Immunol. Allergy Clin. North. Am.,* 2004, **24**, 477.
9. G. Choquet-Kastylevsky, T. Vial and J. Descotes, *Curr. Allergy Asthma Rep*., 2002, **2**, 16.
10. S. N. Lavergne, H. Wang, H. E. Callan, B. K. Park and D. J. Naisbitt, *J. Pharmacol. Exp. Ther.*, 2009, **331**, 372.
11. N. Sahu, D. Das, S. Mondal, S. Roy, P. Dutta, N. Sepay, S. Gupta, E. Lopez-Torres and C. Sinha, *New J. Chem.*, 2016, **40**, 5019.
12. N. Farrel, "Transition Metal Complexes as Drugs and Chemotherapeutic Agents", Kluwer, Dordrecht, 1989.
13. C. Pérez, C. V. Díaz-García, A. Agudo-López, V. Solar, S. Cabrera, M. T. Agulló-Ortuño, C. Navarro-Ranninger, J. Alemán and J. A. López-Martín, *Eur. J. Med. Chem.,*

2014, **76**, 360.

14. K. K. Narang, J. K. Gupta and *J. Inorg. Nucl. Chem.*, 1976, **38***,* 589.
15. W. Kaim, B. Schwederski and A. Klein, "Bioinorganic Chemistry-Inorganic Elements in the Chemistry of Life: An Introduction and Guide", 2nd ed., Wiley, New York, 2013.
16. (a) D. Das, N. Sahu, S. Mondal, S. Roy, P. Dutta, S. Gupta, T. K. Mondal and C. Sinha, *Polyhedron,* 2015, **99**, 77; (b) S. Mondal, S. M. Mandal, T. K. Mondal and C. Sinha, *Spectrochem. Acta Part A,* 2015, **215**, 268.
17. (a) A. I. Vogel, "A Text Book of Quantitative Inorganic Analysis : Theory and Practice", 2nd ed., Longmans Green & Co., New York, 1951, p. 344; (b) A. I. Vogel, A. R. Tatchell, B. S. Furnis and A. J. Hannaford, "Vogel's Textbook of Practical Organic Chemistry", 5th ed., Longman, 1996.
18. G. A. Bain and J. F. Berry, *J. Chem. Ed*., 2008, **85**, 532.
19. L.E. Vidal Salgado and C. Vargas-Hernandez, *Am. J. Anal. Chem*., 2014, **5**, 1290.
20. Bruker, Program name.Bruker AXS Inc., Madison, Wisconsin, USA, 2001.
21. R. H. Blessing, *Acta Cryst. A,* 1995, **51**, 33.
22. G. M. Sheldrick, *Acta Cryst. A,* 2008, **64**, 112.
23. L. J. Farrugia, *J. Appl. Cryst.,* 1997, **30**, 565.
24. G. M. Sheldrick, *Acta Cryst. A*, 2014, **70**, C1437.
25. G. M. Sheldrick, *Acta Cryst. A*, 2008, **64**, 112.
26. "International Tables for Crystallography", ed. A. J. C. Wilson, Kluwer Academic Publishers, Dordrecht, Netherlands, Table 6.1.1.4, 1992, **C**, 572.
27. J. A. Ibers and W. C. Hamilton, *Acta Crystallogr*., 1964, **17**, 781.
28. D. C. Creagh and W. J. McAuley, "International Tables for Crystallography", ed. A. J. C. Wilson, Kluwer Academic Publishers, Boston, Table 4.2.6.8, 1992, **C**, 219.
29. D. C. Creagh and J. H. Hubbell, "International Tables for Crystallography", Vol. C, ed. A. J. C. Wilson, Kluwer Academic Publishers, Boston, Table 4.2.4.3, 1992, **C**, 200.
30. CrystalStructure 4.2: Crystal Structure Analysis Package, Rigaku Corporation (2000-2015). Tokyo, Japan.
31. L. J. Farrugia, *J. Appl. Cryst*., 1999, **32**, 837.
32. M. K. Paira, T. K. Mondal, D. Ojha, A. M. Z. Slawin, E. R.T. Tiekink, A. Samanta and C. Sinha, *Inorg. Chim. Acta*, 2011, **370**, 175.
33. A. M. A. Adam, M. Salman, T. Sharshar and M. S. Refat, *Int. J. Electrochem. Sci.,* 2013, **8**, 1274.
34. P. J. Hay and W. R. J. Wadt, *J. Chem. Phys.*, 1985, **82**, 299.
35. M. J. Frisch, G. W. Trucks, H. B. Schlegel, G. E. Scuseria, M. A. Robb, J. R. Cheeseman, G. Scalmani, V. Barone, B. Mennucci, G. A. Petersson, H. Nakatsuji, M. Caricato, X. Li, H. P. Hratchian, A. F. Izmaylov, J. Bloino, G. Zheng, J. L. Sonnenberg, M. Hada, M. Ehara, K. Toyota, R. Fukuda, J. Hasegawa, M. Ishida, T. Nakajima, Y. Honda, O. Kitao, H. Nakai, T. Vreven, J. A. Montgomery (Jr.), J. E. Peralta, F. Ogliaro, M. Bearpark, J. J. Heyd, E. Brothers, K. N. Kudin, V. N. Staroverov, R. Kobayashi, J. Normand, K. Raghavachari, A. Rendell, J. C. Burant, S. S. Iyengar, J. Tomasi, M. Cossi, N. Rega, J. M. Millam, M. Klene, J. E. Knox, J. B. Cross, V. Bakken, C. Adamo, J. Jaramillo, R. Gomperts, R. E. Stratmann, O. Yazyev, A. J. Austin, R. Cammi, C. Pomelli, J. W. Ochterski, R. L. Martin, K. Morokuma, V. G. Zakrzewski, G. A. Voth, P. Salvador, J. J. Dannenberg, S. Dapprich, A. D. Daniels, Ö. Farkas, J. B. Foresman, J. V. Ortiz, J. Cioslowski and D. J. Fox, GAUSSIAN 09, Revision D.01, Gaussian Inc., Wallingford, CT, 2009.
36. A. Frisch, A. B. Nielson and A. J. Holder, GAUSSVIEW User Manual, Gaussian Inc, Pittsburgh, PA, 2000.
37. P. J. Hay and W. R. Wadt, *J. Chem. Phys.,* 1985, **82**, 270.
38. W. R. Wadt and P. J. Hay, *J. Chem. Phys.,* 1985, **284**, 284.
39. M. E. Casida, C. Jamorski, K. C. Casida and D. R. Salahub, *J. Chem. Phys.,* 1998, **108**,1439.
40. V. Barone and M. Cossi, *J. Phys. Chem. A*, 1998, **102**, 1995.
41. M. Cossi and V. Barone, *J. Chem. Phys*., 2001, **115**, 4708.
42. M. Cossi, N. Rega, G. Scalmani and V. Barone, *J. Comput. Chem*., 2003, **24**, 669.
43. Discovery Studio 3.5 is a product of AccelrysInc, San Diego, CA, USA.
44. S. Tabassum, M. Afzal and F. Arjmand, *Eur. J. Med. Chem*., 2014, **74**, 694.
45. P. Leeson, *Nature*, 2012, **481**, 455.
46. P. K. Ojha and K. Roy, *Eur. J. Med. Chem.,* 2010, **45**, 4645.
47. A. Datta, K. Das, C. Massera, J. K. Clegg, C. Sinha, J.-H. Huang and E. Garribba, *Dalton Trans.,* 2014, **43**, 5558.
48. A. Mai-Prochnow, M. Clauson, J. Hong and A. B. Murphy, *Sci. Rep.,* 2016, **6**, 38610.
49. (a) K. Mudasir, D. H. Wijaya, N. Tjahjono, H. Yoshioka and Z. Inoue, *Naturforsch*., 2004, **59b**, 310; (b) M. Navarro, E. J. Cisneros-Fajardo, M. Fernandez-Mestre, D. Arrieche and E. Marchan, *J. Biol. Inorg. Chem*., 2003, **8**, 401; (c) R. B. Nair, E. S. Teng, S. L. Kirkl and C. J. Murphy, *Inorg. Chem.*, 1998, **37**, 139.
50. A. Scozzafava, T. Owa, A. Mastrolorenzo and C. T. Supuran, *Curr. Med. Chem.*, 2003, **10**, 925.
51. L. Z. Benet, C. M. Hosey, O. Ursu and T. I. Oprea, *Adv. Drug. Deliv. Rev*., 2016, **101**, 89.